Accepted: 30 November 2022

DOI: 10.1002/lsm.23624

CLINICAL REPORTS

Low-fluence treatment with a novel fractionated 2,910-nm fiber laser improves photodamage

Eric F. Bernstein MD[1] | **James F. Sanzo PhD**[2] | **Jennifer Y. Wang BA**[3] | **Samuel M. Cotsarelis**[1] | **Mario DiLeonardo MD**[1]

[1]Main Line Center for Laser Surgery, Ardmore, Pennsylvania, USA

[2]Departments of Bioengineering and Pathology, Confocal and Multiphoton Imaging Core Laboratories, University of Pennsylvania, Philadelphia, Pennsylvania, USA

[3]College of Medicine, SUNY Downstate Health Sciences University, Brooklyn, New York, USA

Correspondence

Eric F. Bernstein, MD, MSE, Main Line Center for Laser Surgery, 32 Parking Plaza, Suite 200, Ardmore, PA 19003, USA.
Email: dermguy@dermguy.com

Abstract

Background: Facial rejuvenation by lasers that target water has been a mainstay of esthetic laser treatments for decades. Modern lasers more commonly treat a fraction of the skin surface using ablative, semi-ablative, or nonablative pulses.

Methods: Twenty subjects with visible evidence of chronic photoaging on the face were enrolled in this study. All subjects received two full-face, single-pass treatments spaced 2 months apart with the superficial mode of a 2910 nm fiber laser with an estimated penetration depth of 10 μm, 25% coverage, delivered in a 15 mm × 15 mm square microbeam pattern. A blinded comparison of pretreatment and 3-month post-treatment images was performed. Evaluation of biopsy samples for laser-tissue effects was performed on three separate subjects and biopsies were harvested 1-day post-treatment, 1-week post-treatment, and 2-weeks post-treatment.

Results: Blinded evaluation of digital images revealed an average improvement score of 25.1 ± 14.5 (mean ± SEM) or 25.1%, using an 11-point scale evaluating overall improvement in photoaging ($p < 0.001$). Post-treatment effects were limited to mild-to-moderate erythema and edema, and the pain was rated a 1.9 out of a maximum of 10. Histology demonstrated superficial changes in the stratum corneum and epidermis with dermal inflammation present at 1-day post-treatment and 1-week post-treatment, with a return to baseline at 2 weeks.

Conclusions: The 2910 nm fiber laser is safe and effective for improving mild photodamage, with minimal discomfort and downtime. Dermal inflammation results from very superficial epidermal injury and may contribute to clinical improvement.

KEYWORDS

2910 nm, fiber laser, fractionated, histology, photoaging, skin

INTRODUCTION

In this study, we investigate for the first time a 2,910 nm erbium:glass (Er:glass) fiber laser for improving mild photodamage, using a superficial treatment mode. Due to the wavelength, beam profile, fiber laser platform, and small treatment beam diameter, the new 2,910 nm fiber laser delivers clinical results with minimal pain and downtime, fast treatment times, and the versatility of functioning in superficial mode, deep mode, or a combined mode. Lasers targeting water to various degrees have been used in both full-field and fractionated modes for decades to improve cutaneous photoaging. Carbon dioxide (CO_2) lasers were the first such lasers used in treating photodamage,[1–3] but often result in unacceptable side effects for many potential patients.[4] Thus, less-ablative and nonablative fractionated lasers were developed to reduce recovery times while still

providing clinical benefits. Lasers operating at the mid-infrared 1,440, 1,550, and 1,927 nm wavelengths, which penetrate more superficially, have been shown to produce less epidermal injury and reduced residual thermal damage in the dermis.[5–8] These lasers are typically administered in a series of treatments as opposed to more ablative lasers, such as CO_2 lasers, which are often administered in a single treatment. Because CO_2 lasers typically ablate the epidermis while leaving a relatively thick layer of thermally altered dermal collagen behind, the mid-infrared lasers are used for more superficial treatments and leave much less residual thermal damage. Less thermal damage results in reduced downtime, but more gradual improvement, generally requiring a series of treatments. Fractionated lasers deliver treatment to only a portion of the skin surface area, limiting laser treatment zones to reduce side effects, downtime and discomfort, while still inducing inflammation across the entire treated area. Along with a high safety profile and a rapid healing time, good cosmetic results have been achieved from fractionated nonablative and semi-ablative lasers treating fine lines and wrinkles, and unwanted pigmentation, as well as being used to enhance penetration of topicals.[9–16] Water absorption in the skin is highest between 2,900 and 3,100 nm, resulting in tissue ablation with very little residual thermal damage,[17–19] thus resulting in less side effects and downtime than nonfractionated or ablative fractionated lasers. Here, we investigate a new, fractionated, 2,910 nm, Er:glass fiber laser, with a unique beam profile and small beam diameter, using the superficial treatment mode for its effect on mildly photodamaged skin. We evaluate improvement in photoaging, side effects, and the histology of treated skin 1-day following treatment, 7-days following treatment, and 14-days following treatment.

MATERIALS AND METHODS

Subjects

Potential subjects for this Institutional Review Board-approved study were initially screened by the treating physician for the five key signs of photoaging: fine lines and wrinkles, enlarged pores, sagging skin, telangiectasias, and hyperpigmentation. Twenty subjects rated by the treating physician to have mild photodamage were selected for laser treatment and enrolled in the study. Three additional subjects receiving treatment of non-photodamaged skin followed by skin biopsies taken 1-day following laser treatments, 1-week following laser treatments, and 2-weeks following laser treatments, were enrolled without assessment of photodamage, since biopsies were performed on sun-protected skin. All enrolled subjects completed the study. Clinical study participants receiving facial laser treatments consisted of 4 males and 16 females and ranged in age from 24 to 60 years, with a mean age of 46.1 ± 11.7 years (mean ± SD), with clinically identifiable chronic photoaging on the face. The study was open to all Fitzpatrick skin types with two enrolled subjects having skin type I, seven with skin type II, nine with skin type III, and three with skin type IV. The three subjects receiving laser treatment and skin biopsies were not assessed for photodamage, as sun-protected skin was biopsied, and were 57, 68, and 47 years old and had skin types II, III, and IV, respectively. Subjects receiving facial laser treatments, injectable fillers, or neurotoxins, taking isotretinoin within 6 months of the start of the study, who had dermatitis or dermatosis in the treatment area, or a history of keloid formation were excluded.

Laser

The laser used in this study was a mid-infrared, Er:glass, 2,910 nm fiber laser (UltraClear; Acclaro Medical). The laser energy is administered through a laser fiber, and not an articulated arm. The laser beam is focused on a microbeam spot size of 170 μm, and these microbeams are arranged in an annulus forming a "spot" composed of 33 microbeams. The spot has a gaussian cross section consistent with other single-mode, high-beam-quality lasers. Microbeams are delivered in an annular array with a 35% fixed spot overlap to create an even energy distribution over the entire annulus, or spot. The microbeams overlap so that the troughs of the Gaussian beam are additively delivering very uniform energy for the laser spot (Figure 1). The setting used for this clinical study arranged the microbeams in an annular ring formation using 33 microbeam pulses per ring, producing an annulus that is 0.17 mm thick and 1.20 mm in diameter. For this study, a 15 mm × 15 mm square pattern was selected from a variety of pattern options and generated using a computer pattern generator, placing 81 rings in a 9 × 9 ring pattern (Figure 2). The number of rings per unit area was selected by choosing a density setting of 25%, determining that to achieve 25% coverage of the 15 mm × 15 mm treatment area required even placement of 81 rings, 1.50 mm apart, across the square pattern. The overall energy per pattern was 1.8 ± 0.1 J, using 2,673 individual microbeams, each with an energy of 0.6 mJ per microbeam. Thirty-three microbeams form an annular spot resulting in an annular spot energy of 21.5 mJ/spot, or ring. The overall time to deliver one 15 mm × 15 mm square pattern was 0.7 seconds, with a fluence of 2.5 J/cm^2 for each 15 mm × 15 mm treatment pattern. These settings result in a predicted ablation depth of 10 ± 1.5 μm.

For histology treatment areas, treatment settings of 20 and 60 μm were used corresponding to microbeam energies of 1.3 and 3.9 mJ, and 42.9 and 128.7 mJ/spot or annular ring, respectively. Over the 10 mm × 10 mm

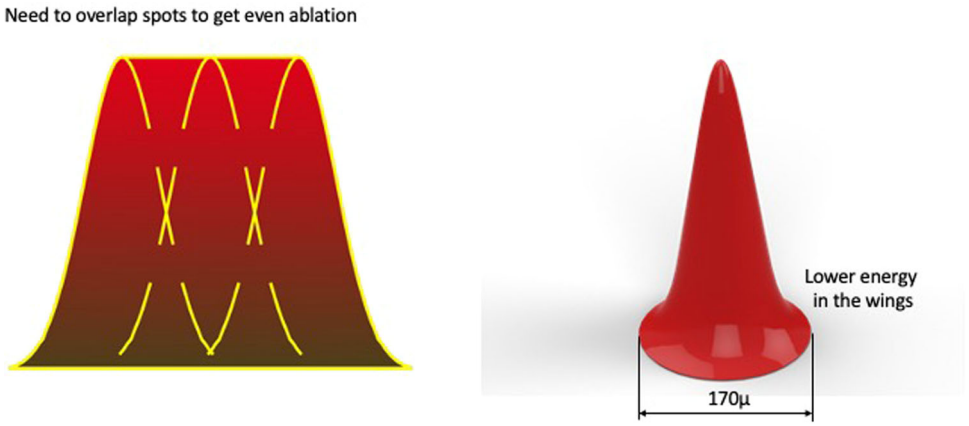

FIGURE 1 Microbeams are overlapped when forming annular pulses comprised of 33 microbeams arranged in a circular pattern, creating a uniform pulse

FIGURE 2 Laser pulses are comprised of 33 microbeam pulses as illustrated here, with an off cycle between microbeams that is longer than the thermal relaxation (TRT) of each microbeam in the treated skin. Annular pulses are delivered in a 15 mm × 15 mm square comprised of 81 ringed pulses delivered in 0.7 seconds.

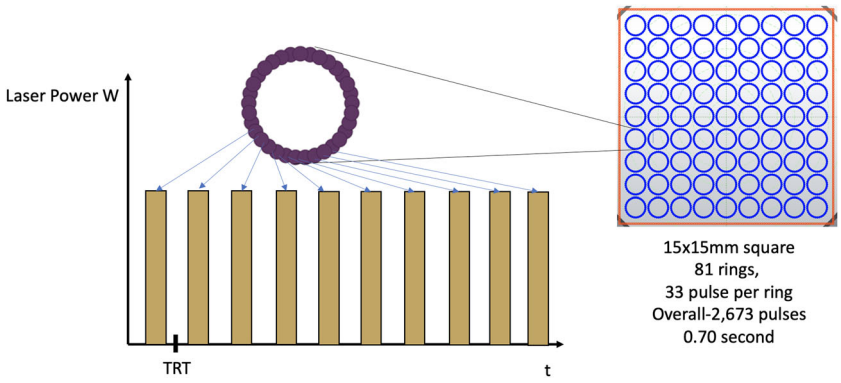

patterns, 36 annular spots were delivered, depositing 1.6 and 4.6 J of energy for the 20 and 60 µm settings, respectively.

Laser treatment

All clinical subjects were treated to their entire face with a single laser pass, for a total of two treatments, spaced 2 months apart, with the 2,910 nm, Er:glass, fiber laser. The treatment energy used in this study was determined by the treating physician based on prior treatments where post-treatment improvement and side effects were observed for a range of treatment energies. Histology studies also contributed to the selection of clinical parameters for this study. An energy setting of 10 µm was used for both treatments, which corresponds to a fluence of 2.5 J/cm^2 over the entire treatment area. The overall energy per pattern was 1.8 ± 0.1 J, using 2,673 individual micro-beams, each with an energy of 0.6 mJ per microbeam. Thirty-three microbeams form an annular spot resulting in an annular spot energy of 21.5 mJ/spot or ring. A square pattern was selected using the maximum available 15 mm × 15 mm treatment area, with a treated area density setting of 25% being selected. To treat 25% of the 15 mm × 15 mm square, 81 annular spots were deposited evenly over the treatment area 1.5 mm apart. Treatments were administered using an automatic repeat mode with a repetition rate of 1.0 Hz. No topical numbing cream was used, and treatment times averaged approximately 5 minutes.

The three subjects receiving laser treatments for histologic evaluation were treated to the lower back skin at six treatment sites, with a seventh site serving as an untreated control. Three sites on each subject were treated as above with a 20 µm setting delivering 5.0 J/cm^2, with 1.3 mJ/microbeam and 43 mJ/spot or annular ring, and 1.6 J per 10 mm square treatment area comprised of 36 evenly spaced annular spots. Three additional sites were treated at a higher setting of 60 µm, corresponding to 15.0 J/cm^2, delivering 3.9 mJ/microbeam, 128.7 mJ/spot or annular ring, and 4.7 J per 10 mm square treatment zone.

Blinded assessment of standardized images

Full-face digital images using standard flash lighting were taken of every subject immediately before treatment and 3 months following the final treatment with a

professional digital imaging system with a standardized head immobilizer to maintain proper head positioning (Visia CR; Canfield Scientific, Inc.). To ensure reproducible head positioning during pre-treatment and post-treatment imaging, the imaging system incorporates digital ghosting of a previous image displayed with real-time movie displays of head position to enable maximal agreement in positioning between pretreatment and post-treatment digital images. The video image is matched to the static ghosted image resulting in the matching of pretreatment and post-treatment positioning. Three facial positions were taken of each subject before and 3 months after treatment including a frontal, 45° angle of the left side of the face, and a 45° angle of the right side of the face view.

The treatment effect was evaluated by three blinded physician evaluators comparing randomized pairs of pre-treatment and 3-month post-treatment images. Evaluators attempted to identify the image they perceived to be the pre-treatment image, and then rated the level of improvement, if any, over the presumed 3-month post-treatment image. Blinded physician evaluators rated the overall improvement in photodamage using an 11-point scale from 0 to 10, where a score of 0 corresponded to no improvement, a score of 1 was a 10% improvement in photodamage, a score of 5 would be a 50% improvement, and a score of 10 would correspond to 100%, or complete improvement in cutaneous photodamage. Incorrectly identifying a post-treatment image as pretreatment resulted in a negative score; for example, a score of 4 would be recorded as a score of −4, or a 40% worsening of the appearance of photodamage.

Subject rating of side effects

Subjects rated erythema, edema, and pinpoint bleeding on a 4-point Likert scale from none (0), to mild (1), moderate (2), and severe (3) immediately following each treatment. Pain during each treatment was rated by subjects using an 11-point (0–10) scale where 0 corresponds to no sensation or some sensation but without any pain, a score of 5 corresponds to moderate pain, to a maximal pain score of 10.

Histologic evaluation

Skin biopsies of two treatment energies and the untreated control site were taken 1-day following treatment for each of the three subjects. A second biopsy was taken 1-week following treatment of each of the two administered energies, and again 2-weeks following laser treatment. Treatment and control sites for biopsy were infiltrated with lidocaine 0.5% with 1:200,000 epinephrine. A 4-mm punch biopsy was performed, sutured with 4-0 nylon sutures, and immediately placed into buffered formalin. Biopsy specimens were sectioned entirely through the specimen in 5 μm slices and then stained with hematoxylin and eosin and placed onto glass slides resulting in 30 slides per specimen with 4–5 tissue sections per slide. Three biopsy specimens, one from each subject, were harvested at each laser energy, as was a single control biopsy, as stated above. All sections were examined, and sections with evidence of maximal laser treatment, representing the presence of a fractionated annular spot, were selected for review. Four tissue sections were then analyzed for each biopsy specimen, each section separated from one other by at least 20 μm in the tissue block. Sections were evaluated and slides were visualized using an Olympus BX43 microscope (Olympus America Inc.) using Olympus ×2, ×4, ×10, ×20, and ×40 objectives. Images of stained sections were acquired with the DP 28 digital camera with 4k resolution (Olympus America Inc.) and ported to an HP Z2 mini G5 workstation (Hewlett-Packard).

The epidermis was evaluated for evidence of laser effect. The destruction of keratinocytes was evaluated, and the average depth of injury was noted in four sections for each biopsy specimen. The stratum corneum was examined and determined to be normal basket weave, parakeratotic evidencing laser tissue effect, or a combination of the two. Evidence of any scale crust was noted. The dermis was evaluated for the extent of inflammation using a 7-point scale with 0= no inflammation, 1 = low-grade mild inflammation, 2 = high-grade mild inflammation, 3 = low-grade moderate inflammation, 4 = high-grade moderate inflammation, 5 = low-grade severe inflammation, and 6 = high-grade severe inflammation.

RESULTS

Evaluation of digital images reviewed by blinded physician observers

All 20 subjects received three treatments; however, a single subject failed to return for final imaging. Of the 19 frontal image sets comprised of frontal and two side views that were evaluated, two subjects had their pretreatment images incorrectly identified by two reviewers and a single subject was incorrectly identified by the third reviewer. In two of the cases, the same images were misidentified. These images were assigned a negative score. The combined accuracy rate for correctly identifying the baseline image was 52 correct out of 57 images or a 91.2% success rate. The average improvement score for the 19 subjects was 25.1 ± 14.4% (mean ± SEM), which was statistically significant ($p < 0.001$) (Figure 3). Reviewers did not disagree with one another in a statistically significant manner (analysis of variance; $p = 0.89$).

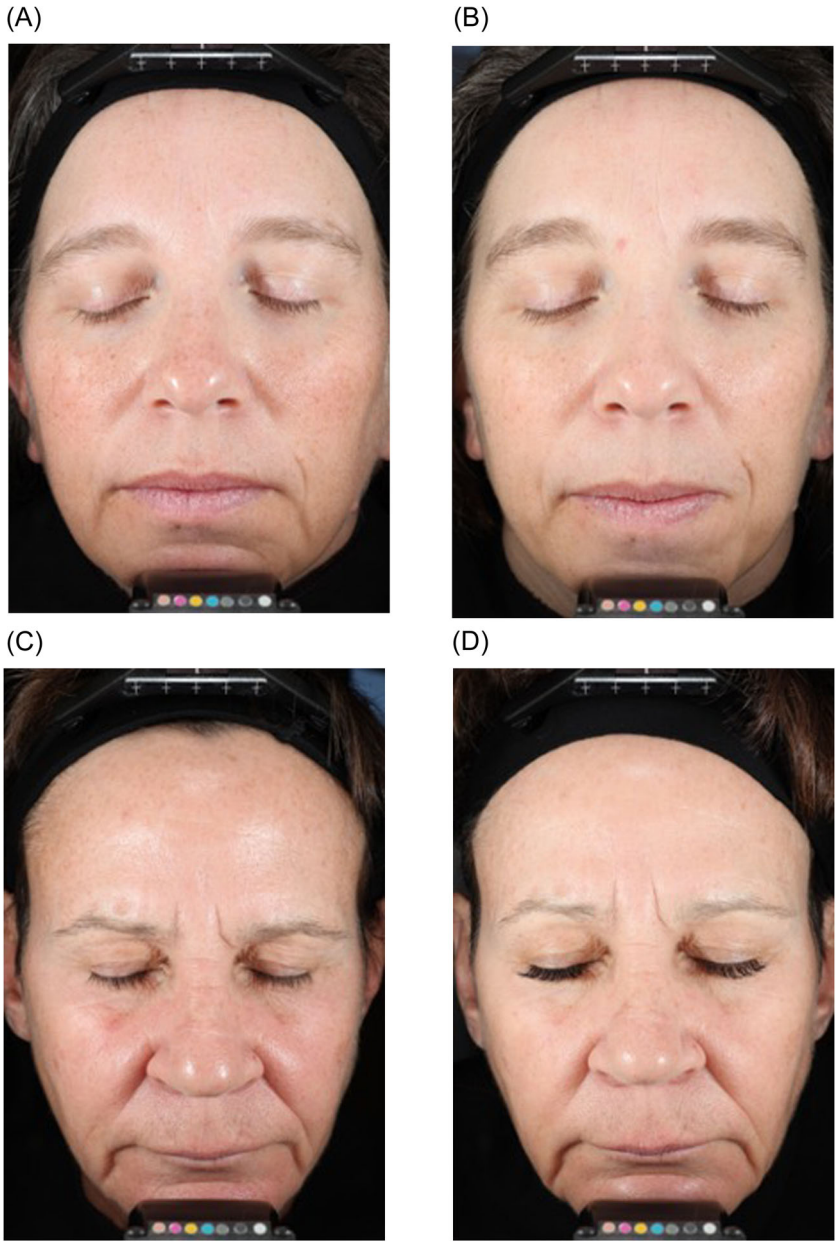

FIGURE 3 Frontal views using standard lighting with showing before (A, C) and 3 months after (B, D) two treatments with the fractionated, Er:glass fiber laser at a low-energy, 10 μm treatment setting.

Side effects of treatment

Pain during treatment, as evaluated on a 0 (none) to maximal pain (10) scale ranged from 0 to 5, averaging a score of 1.8 ± 1.2 (mean ± SD) during the first treatment, ranged from 0 to 5 averaging a score of 2.1 ± 1.4 during the second treatment, and ranged from 0 to 5 and averaged a score of 1.9 ± 1.3 combining both treatments. Subjects only reported pain during treatment with no pain occurring once laser treatment was concluded.

Erythema post-treatment as evaluated on a 0 (none) to 3 (severe) scale ranged from 1 to 3 and averaged 1.8 ± 0.6% (mean ± SD) after Treatment 1, from 1 to 3 and averaged 1.7 ± 0.6% after Treatment 2, and from 1 to 3 and averaged 1.7 ± 0.6% combining the results of both treatments. Post-treatment edema ranged from 0 to 1 and averaged 0.6 ± 0.6% after Treatment 1, from 0 to 2 and averaged 0.9 ± 0.4% after Treatment 2, and from 0 to 2 and averaged 0.7 ± 0.5% combining the results of both treatments. There was no pinpoint bleeding after any treatment. No hyperpigmentation, hypopigmentation, or scarring was noted in any post-treatment image.

Histologic evaluation

20 μm treatment setting

The stratum corneum in control specimens was all normal basketweave orthokeratosis, as expected, with the underlying epidermis demonstrating the typical cellular progression of differentiation to become stratum

corneum as the cells migrate up from the epidermis. An energy level of 1.3 mJ/cm^2 for each microbeam and 42.9 mJ per spot, the 20 μm setting, produced areas of laser effect interspersed with spared areas due to the fractionated nature of the laser pattern. Coagulated areas of stratum corneum were evident 1-day post-treatment, demonstrating flattening and increased eosinophilic staining, alternating with areas of normal orthokeratosis (Figure 4A,B). Seven days following laser treatment, areas of parakeratosis with underlying normal basketweave orthokeratosis were present, indicating that the treated areas were being shed and replaced with normal-appearing stratum corneum after only 1-week post-treatment. The normal basketweave orthokeratosis was present in various thicknesses from a single cellular layer to a more normal-appearing basketweave stratum corneum, with some areas of complete parakeratosis remaining (Figure 4C,D). Specimens were taken from skin treated with the 20 μm setting 14-days after laser treatment often showed areas of parakeratosis with underlying normal basketweave orthokeratosis under all areas of parakeratosis, or some areas with no parakeratosis at all where it had presumably been completely shed revealing normal-appearing orthokeratosis (Figure 4E,F). The epidermis was normal in all specimens, with normal basketweave orthokeratosis in all areas, with or without the overlying parakeratotic stratum corneum that was being shed.

Inflammation in control specimens ranged from 0 to 1 (none to low-grade mild) averaging 0.2 ± 0.2 (mean ± SEM) out of a maximum of 6, and was limited to the papillary dermis when present, but was not present in 7 of 12 specimens examined. In specimens treated with the 20 μm laser setting 1-day post-treatment, the degree of inflammation ranged from low-grade mild in most specimens to high-grade mild in three sections, averaging a score of 1.2 ± 0.2 out of 6, in the low-grade mild range, and was limited to the papillary dermis (Figure 5A,B).

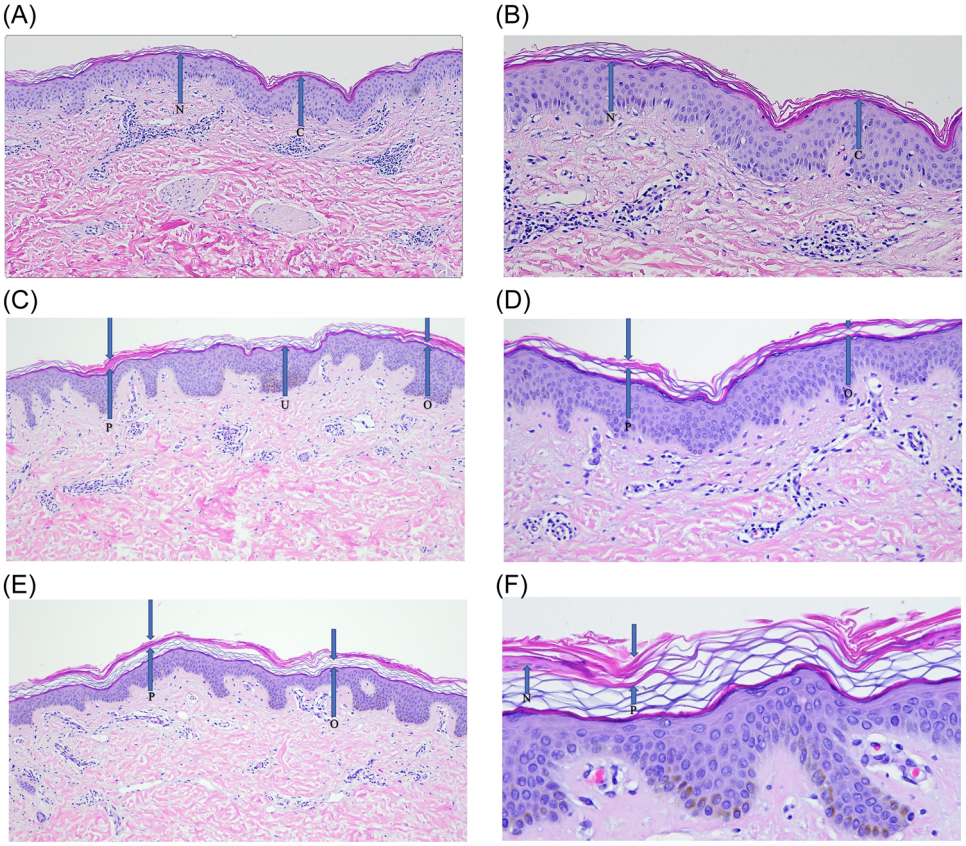

FIGURE 4 (A) Normal (N) untreated and treated/coagulated (C) stratum corneum in skin treated with the lower 20 μm setting, 1-day post-treatment (magnification ×10). (B) The right side of the image shows coagulated stratum corneum (C) with a normal epidermis below while the left side of the image shows an untreated area with normal, basket weave stratum corneum (N) in this specimen 1-day post-treatment with the 20 μm setting (magnification ×20). (C) Seven days post-treatment (×10 magnification) at the 20 μm setting demonstrates new areas of orthokeratotic stratum corneum (O) being formed beneath the treated parakeratotic areas (P) and untreated areas of orthokeratosis (U). (D) A high magnification (magnification ×20) view of an area treated with the low-energy laser setting 7-days post-treatment shows a normal blue-staining basket weave stratum corneum (O) beneath the previously treated pink-staining parakeratotic stratum corneum (P). (E) Fourteen days after low-energy treatment epidermis appears as a pink band of parakeratosis (P) at the top of the specimen, overlying the normal basket weave orthokeratotic stratum corneum (O) that has grown underneath the treated areas (magnification ×10). (F) Higher magnification shows the relationship between the previously laser-treated parakeratotic stratum corneum in pink (P) in contrast to the blue basketweave orthokeratosis below. Nonviable nuclei (N) are present in the parakeratosis as blue elongated structures (magnification ×40).

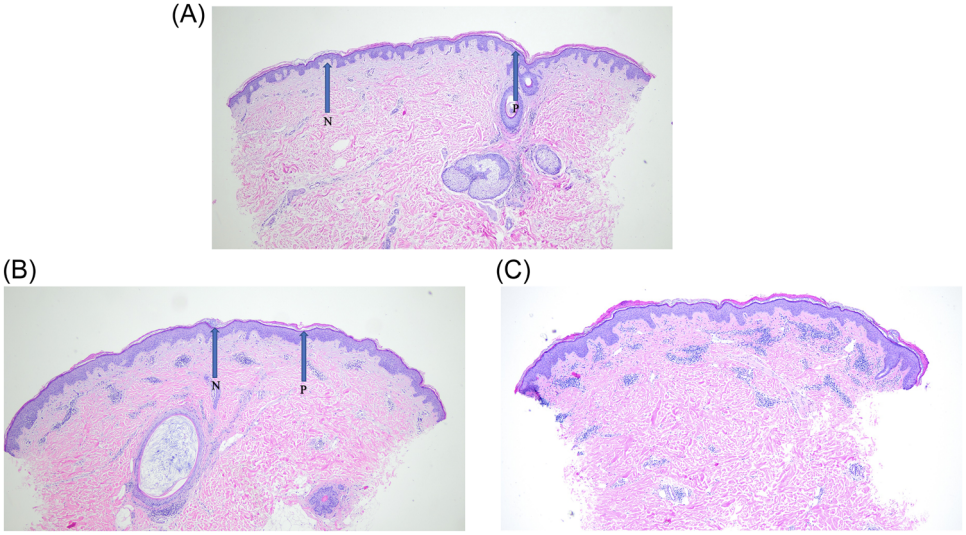

FIGURE 5 (A) A biopsy specimen showing no inflammation (rating 0) with evidence of laser treatment in the stratum corneum showing compact parakeratosis (P) interspersed with untreated areas showing normal basket weave stratum corneum (N), 7-days following low-energy laser treatment (magnification ×4). (B) A biopsy specimen showing inflammation rated as high-mild, with a score of 2, 1-day post-treatment with the low 20 μm setting (magnification ×4). Areas of laser treatment in the stratum corneum show compact parakeratosis (P) interspersed with untreated areas showing normal basket weave stratum corneum (N). (C) Inflammation is present at the level of the superficial reticular dermis (rating 2/6 corresponding to low-grade mild inflammation) in this high-energy (60 μm setting) treated specimen, 7-days following laser treatment (magnification ×4).

Inflammation in skin specimens treated with the 20 μm laser setting, Day-7 post-treatment, demonstrated inflammation ranging from none to low-grade moderate, averaging a score of 0.7 ± 0.5 out of 6, in the low-grade mild range, and occurred primarily in papillary dermis extending to, and sometimes into, the beginning of the reticular dermis. By 14-days post-treatment in low-energy-treated skin, inflammation was not present, and the dermis of skin biopsy samples looked indistinguishable from control specimens. The inflammatory response ranged from none to low-grade mild, averaging a score of 0.2 ± 0.2 out of 6, in the no inflammation range. Most sections showed no inflammation, identical to control samples.

60 μm treatment setting

Skin treated with a microbeam energy 3.9 mJ, and 128.7 mJ/spot or annular ring, which corresponds to the 60 μm setting, 1-day after laser treatment demonstrated coagulation of the superficial-to-mid epidermis, evidenced by diffuse eosinophilic staining and loss of cellular architecture, interspersed with skip areas of the normal, untreated epidermis due to the fractionated nature of the laser grid. The coagulated epidermis was hypereosinophilic with small, pyknotic blue-staining nuclei. The overlying stratum corneum was absent in treated zones (Figure 6A,B). In some areas, inflammatory cells were seen in the epidermis. There were a few areas where the laser effect on the epidermis extended to the basal layer of the epidermis but not beyond it. No coagulation was seen in the dermis in any specimens. Seven days after treatment, skin treated with the 60 μm setting demonstrated areas of parakeratosis with underlying normal basketweave orthokeratosis, indicating that the treated areas were being shed and replaced with normal-appearing stratum corneum after 1-week post-treatment. The normal basketweave orthokeratosis was present in various thicknesses from a single cellular layer to a more normal-appearing basketweave stratum corneum a few cell layers thick, but with some areas of complete parakeratosis remaining. Normal unaffected areas were present between the treatment zones due to the fractionated nature of laser distribution (Figure 6C,D). In skin treated with the 60 μm setting 14-days post-treatment, the epidermis was all perfectly normal as in the 60 μm 7-day post-treatment and control specimens. The stratum corneum was a normal basketweave orthokeratosis across the entire epidermis in virtually all specimens, with only a few areas of retained parakeratosis. Some specimens had a normal-thickness stratum corneum while many had a thinner, orthokeratotic stratum corneum (Figure 6E,F).

Inflammation in skin specimens treated with the 60 μm laser setting 1-day post-treatment demonstrated inflammation ranging from low-grade mild to low-grade moderate averaging a score of 2.2 ± 0.4 out of 6, in the high-grade mild range, and occurred primarily in papillary dermis extending to, and sometimes into, the beginning of the reticular dermis. By 7-days post-treatment inflammation ranged from low-grade mild to low-grade moderate averaging a score of 1.9 ± 0.4 out of 6, in the high-grade mild range, and occurred primarily in

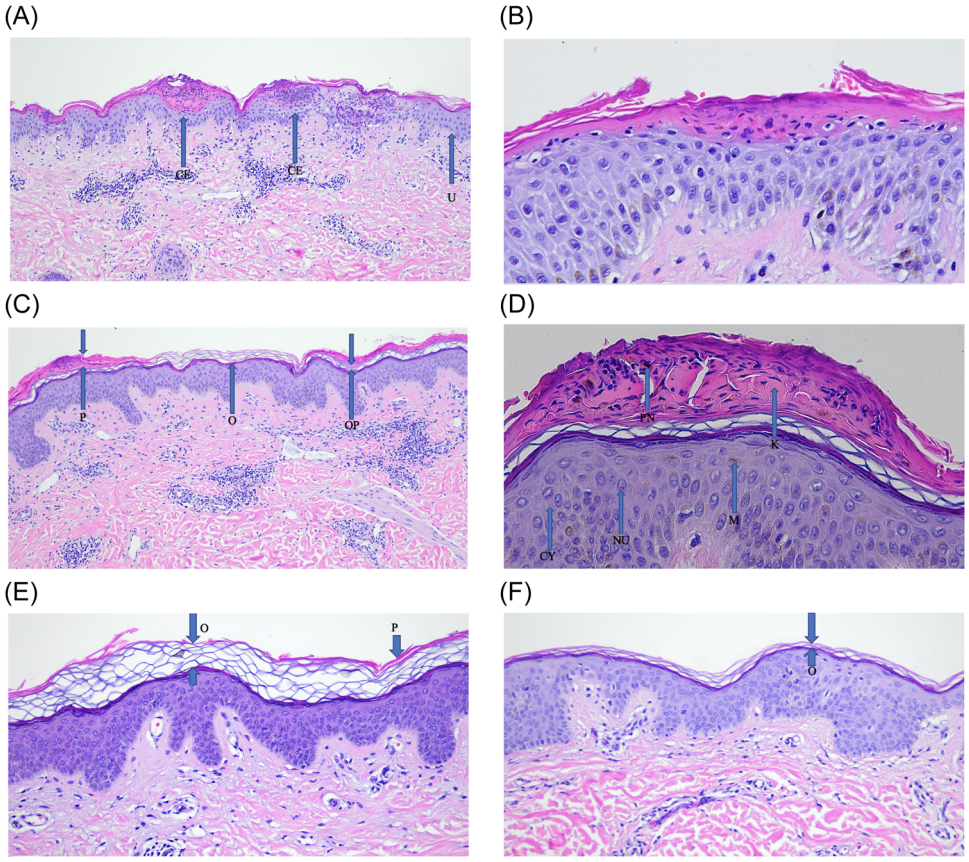

FIGURE 6 (A) Skin treated with the high-energy (60 μm) setting, 1-day post-treatment (×10 magnification) demonstrates areas of the upper half of the epidermis showing coagulation with eosinophilic staining of the affected area and pyknotic nuclei (CE) with an area of untreated, the adjacent epidermis (U). This laser is fractionated creating untreated skip areas alternating with treated ones. (B) A high magnification (magnification ×40) view of a zone of epidermal coagulation 1-day post-treatment with the high-energy setting shows eosinophilic staining of the top 1/3 of the epidermis with pyknotic nuclei indicative of laser effects. The underlying epidermis is intact with normal-appearing nuclei. (C) Areas of normal, untreated orthokeratotic stratum corneum (O) are interspersed with areas of thick parakeratosis (P) in this high-energy-treated specimen, 7-days post-treatment (magnification ×10). The parakeratosis seen in high-energy-treated specimens is thicker than that of low-energy-treated specimens due to the greater volume of stratum corneum and underlying epidermis affected by higher energy treatments. Treated parakeratotic areas have underlying normal orthokeratosis (OP) that have been replaced by 7-days post-treatment. (D) This very high-power image (magnification ×40) shows pyknotic nuclei (PN) that stain dark blue from laser-treated epidermal cells that are now shedding above a normal, fully recovered epidermis and basketweave stratum corneum. The pink-staining material is keratin (K) from the laser-treated epidermal cells and stratum corneum that are now being shed. Keratinocytes with normal, healthy nuclei (NU) surrounded by lighter-staining purple cytoplasm (CY). Melanin pigment (M) is seen in this subject with Fitzpatrick skin type III. (E) A skin biopsy specimen treated with a high-energy setting 14-days following treatment (×20 magnification) showing thin areas of retained parakeratosis (P) overlying normal orthokeratosis (O). (F) Skin treated with the high 60 μm setting 14-days following treatment (×20 magnification) showing a thinned, orthokeratotic stratum corneum (O).

papillary dermis extending to, and sometimes into, the beginning of the reticular dermis (Figure 5C). As with 20 μm treated skin 14-days post-treatment, inflammation was not present and resembled untreated control specimens. The inflammatory response ranged from none to low-grade mild, averaging a score of 0.3 ± 0.3 out of 6, in the no inflammation range, resembling untreated control specimens.

DISCUSSION

In this study, we investigated the clinical and histologic effects of a new, fractionated 2,910 nm Er:glass fiber laser delivering fractionated arrays of microbeams to create microscopic thermal treatment zones within the stratum corneum and epidermis using the superficial setting. Laser energy is delivered through a laser fiber, and not an articulated arm, to a reusable aluminum handpiece. The 2,910 nm fractionated laser resulted in statistically significant clinical improvement of cutaneous photodamage, with minimal discomfort and side effects, as evaluated by blinded physician evaluators rating standardized digital images. Despite minimal-to-no discomfort, clinical erythema and edema immediately post-treatment were typically mild to moderate, indicative of a clinically evident inflammatory response which presumably contributed to the clinical improvement. Despite the very minimal histologic evidence of epidermal injury at twice the treatment energy used in the

current study, post-treatment erythema and edema were mild to moderate. Histologic studies were performed as a prelude to clinical treatments and treatment energy below the minimum energy used in histology studies was selected due to preliminary treatments using a 10 μm setting eliciting a uniform erythema response with minimal-to-no discomfort and significant patient satisfaction. It is presumed that histologic examination of energies lower than that used in the current study would demonstrate even less epidermal injury than noted in the current study.

The potential advantages of the 2,910 nm fiber laser used in the current study over other ablative, semiablative, and nonablative lasers are due to the characteristics of this unique device. First, the 2,910 nm wavelength is strongly absorbed by water, resulting in ablation with very little thermal energy deposition in the skin. This enables the removal or alteration of very precise layers of tissue in the stratum corneum, epidermis, or dermis. Other lasers operating at 2,940 nm have similar absorption in water; however, those lasers are flashlamp-driven erbium:YAG (Er:YAG) lasers that emit laser energy at a much slower repetition rate than our current device and do not have the ability to deliver the very low energies necessary for very superficial ablation. An early and very large study of 250 subjects demonstrated the ability of the Er:YAG laser operating at 2,940 nm to deliver superficial resurfacing using topical anesthetic in all subjects with significantly less downtime than had been possible with earlier-generation CO_2 lasers, providing some of the first, strong, positive data for use of wavelengths at this peak of water absorption.[18] The Er:glass fiber laser used in the current study can administer pulses in the 3,000–5,000 Hz range, thus enabling the delivery of very uniform annular spots comprised of 33 overlapping microbeams. This overlap enables the lower energy shoulders of each beam to add up to the same energy as is present in the center of the beam, for a uniform spot with consistent tissue effects. In addition, the laser is extremely fast, and the uniformity and highly water-absorbing wavelength at 2,910 nm results in very low discomfort combined with rapid healing times. While the current Er:glass fiber laser can operate in superficial mode, drilling mode, or a combination of the two, this study utilized only the superficial mode and studied its effects on mildly photoaged skin. Patients demonstrated highly statistically significant clinical improvement as evaluated by blinded physicians rating digital images, and a very low pain score rating in the absence of any topical anesthetic, combined with very short treatment times averaging 5 minutes when treated with this unique laser.

Other water-targeting lasers such as the ablative CO_2 laser, or the high-powered nonablative 1,550 nm Er:glass laser, and the 1,927 nm thulium fiber laser are less strongly absorbed by water than the current device, and thus result in more residual thermal damage, discomfort, and downtime when achieving equivalent amounts of ablation. These lasers are used extensively for the treatment of photodamage and acne scarring and have been for many years.[20–24] More recently, the low-energy 1,440 and 1,927 nm nonablative and semiablative fractionated diode lasers have been widely adopted for delivery of superficial treatments with less downtime than the corresponding higher powered devices, for mild facial rejuvenation, maintenance of other laser treatment effects, to augment the effect of topical products, and improve many signs of photoaging including hyperpigmentation.[12–16] Even at low fluences, the low-energy 1,440 and 1,927 nm fractionated lasers create a zone of dermal damage, as evidenced by altered collagen staining, in a semicircular zone at the base of each fractionated microbeam.[9] The 2,910 nm laser used in the current study is capable of extremely superficial treatment with little-to-no epidermal injury evidenced on histology, as well as ablating the stratum corneum and altering the cellular architecture of the epidermis at high fluences. What is novel about this device is the ability to create clinical improvement and dermal inflammation that presumably leads to this improvement, while only creating very superficial epidermal or stratum corneum changes on histologic examination. The mechanisms for the inflammation resulting from such superficial changes on histologic examination remain to be elucidated but are likely multifactorial including alteration of skin barrier function, communication of epidermal nerve fibers with the underlying dermis, as well as cytokine release from keratinocytes affecting the underlying dermis. Investigation of the molecular changes occurring in skin treated with the 2,940 nm Er:YAG laser showed increases in cytokines including interleukins, as well as elevation of AP-1 transcription factors, upregulation of matrix metalloproteinases, and increased expression of types I and III collagen, all with only intraepidermal injury and no disruption of the basement membrane zone.[19] As expected in the current study, increasing the delivered fluence created a greater effect on the epidermis, and further increases in fluence should result in even greater effects with the superficial mode used here, while changing to deep mode enables the creation of dermal microchannels of any depth by changing the beam profile and administered fluence. These modes can be combined in a single treatment pattern with varying fluences enabling a large range of treatment settings that can be tuned to a variety of clinical settings. In this current study, we investigated the clinical effect of very superficial treatment, demonstrating clinical improvement with very little discomfort or downtime.

We also showed histologic evidence of laser treatment in the epidermis at both the 20 and 60 μm settings, with epidermal and dermal changes being measured 1-day post-treatment and 7-days post-treatment, returning to normal in most specimens by 14-days post-treatment. Affected stratum corneum or superficial-to-mid epidermis

remained in place and was slowly shed over the course of 14 days, presumably corresponding clinically to mild scaling or dryness post-treatment. The degree of inflammation present at the 20 μm setting was mild but measurable up to a week after treatment. We postulate that this inflammatory response contributes to the clinical improvement measured in this study. At the higher 60 μm treatment setting used for histologic evaluation, greater inflammation was seen than at the lower setting 7-days following treatment, with skin treated at both energies returning to baseline by 14-days post-treatment. What was striking in this study was the degree of inflammation measured histologically in the dermis in response to very subtle changes in the stratum corneum or epidermis. In the current study, we elected to treat subjects with an energy that was half the lowest fluence used for histology studies, which were performed before the clinical studies, to determine the tissue effects of laser treatment and help direct the selection of clinical parameters with this new device. Clinical erythema following treatment was present in all subjects providing evidence of an inflammatory response even at this lower 10 μm treatment setting, and edema was mild but noted in most subjects immediately following treatment, providing further clinical evidence of an inflammatory response. Presumably, the histologic effect of this lower energy would be similar to, or less than, that measured in the current study investigating histologic effects at two times and six times the treatment fluence. What's remarkable about this is that the histologic effects of laser treatment at the lower 20 μm setting 1-day after treatment were mostly limited to the stratum corneum (Figures 4A,B); however, by 7-days post-treatment, a layer of affected stratum corneum and epidermis (as evidenced by parakeratotic nuclei) was visible (Figures 4C,D).

We measured the tissue effects of this laser using microbeams delivering 5.0 and 15.0 J/cm^2, for the 20 and 60 μm settings, respectively. There was very superficial stratum corneal residual thermal damage at the former setting and stratum corneal and epidermal ablation with greater residual thermal damage at the latter (Figures 4 and 6). Again, treatments in the current study were administered with the superficial mode and produced very precise and limited effects in the epidermis, leaving the dermis unaffected by visible changes in staining at settings up to sixfold higher than used to treat subjects in the current study. Despite the absence of histologic changes to dermal collagen in any specimen, there was a mild and distinct inflammation in the dermis 1-day and 1-week after treatment at the lower 20 μm treatment setting, and at the higher 60 μm setting a more pronounced inflammatory response in the dermis was present.

Ross' group investigated the tissue effects of a pixilated 2,940 nm laser, a similar wavelength as used in the current study, on swine skin with a laser delivering 200 μm-diameter microbeams delivered in 49 or 81 microbeam arrays over an 11 × 11 mm square macropulse, but in drilling mode, not the superficial mode used in the current study. They found no ablation or residual thermal damage, as evidenced by a change in dermal staining characteristics, at 1.9 mJ/microbeam, but did find residual thermal damage without ablation when treated with 3.5 mJ/microbeam. At the latter energy, flattening of the stratum corneum and damage to keratinocytes in the upper third of the epidermis were seen. They saw ablation at an energy of 6.2 mJ/microbeam with residual thermal damage as well,[25] documenting thresholds for residual thermal damage and ablation with this wavelength in drilling mode with increasing fluences.

This study demonstrates that treatment with this new Er:glass fiber laser improves the appearance of photodamaged skin with very little discomfort in the absence of any topical anesthetic, moderate post-treatment erythema and edema indicating a dermal response to treatment, and no other side-effects. Histologic analysis performed on specimens treated at two energy levels demonstrated very superficial residual epidermal damage 1-day following treatment at the base of the stratum corneum in response to the lower treatment setting, and superficial-to-mid residual thermal damage in the epidermis at the higher setting. Dermal inflammation lasting a week in both low-energy and high-energy settings was noted, with greater inflammation in the higher energy setting. Future studies investigating both clinical and histologic changes at higher energy settings in superficial mode, various energies in drilling mode, and the effect of combination modes will further characterize and explore the capabilities of this versatile fiber laser.

CONFLICT OF INTEREST

This study was partially supported through the loan of the study device by Acclaro Medical Inc., the makers of the device used in this study, and funding to support the study. Dr. Eric F. Bernstein is the Chief Medical Officer of Acclaro Medical and holds equity in Acclaro Medical Inc.

ORCID

Eric F. Bernstein http://orcid.org/0000-0002-8202-7893

REFERENCES

1. Ross EV, Grossman MC, Duke D, Grevelink JM. Long-term results after CO_2 laser skin resurfacing: a comparison of scanned and pulsed systems. J Am Acad Dermatol. 1997;37:709–18.
2. Fitzpatrick RE, Goldman MP, Satur NM, Tope WD. Pulsed carbon dioxide laser resurfacing of photoaged facial skin. Arch Dermatol. 1996;132:395–402.
3. Kirsch KM, Zelickson BD, Zachary CB, Tope WD. Ultrastructure of collagen thermally denatured by microsecond domain pulsed carbon dioxide laser. Arch Dermatol. 1998;134:1255–9.
4. Nanni CA, Alster TS. Complications of carbon dioxide laser resurfacing. an evaluation of 500 patients. Dermatol Surg. 1998;24:315–20.

5. Alexiades-Armenakas MR, Dover JS, Arndt KA. The spectrum of laser skin resurfacing: nonablative, fractional, and ablative laser resurfacing. J Am Acad Dermatol. 2008;58(5):719–37.
6. Geronemus RG. Fractional photothermolysis: current and future applications. Lasers Surg Med. 2006;38:169–76.
7. Manstein D, Herron GS, Sink RK, Tanner H, Anderson RR. Fractional photothermolysis: a new concept for cutaneous remodeling using microscopic patterns of thermal injury. Lasers Surg Med. 2004;34:426–38.
8. Narurkar VA, Alster TS, Bernstein EF, Lin TJ, Loncaric A. Safety and efficacy of a 1550nm/1927nm dual wavelength laser for the treatment of photodamaged skin. J Drugs Dermatol. 2018;17:41–6.
9. Friedman PM, Polder KD, Sodha P, Geronemus RG. The 1440 nm and 1927 nm nonablative fractional diode laser: current trends and future directions. J Drugs Dermatol. 2020;19(8):s3–11.
10. Marmon S, Shek SYN, Yeung CK, Chan NPY, Chan JC, Chan HHL. Evaluating the safety and efficacy of the 1,440-nm laser in the treatment of photodamage in asian skin. Lasers Surg Med. 2014;46:375–9.
11. Croix J, Burge S, Chwalek J, Gmyrek R, Chapas A. Split-sided chest study of skin rejuvenation comparing low-energy, 1927-nm thulium fractional laser treatment prior to photodynamic therapy versus photodynamic therapy alone. Lasers Surg Med. 2020;52:53–60.
12. Geddes ERC, Stout AB, Friedman PM. Retrospective analysis of the treatment of melasma lesions exhibiting increased vascularity with the 595-nm pulsed dye laser combined with the 1927-nm fractional Low-Powered diode laser. Lasers Surg Med. 2017;49:20–6.
13. Bae YSC, Rettig S, Weiss E, Bernstein L, Geronemus R. Treatment of post-inflammatory hyperpigmentation in patients with darker skin types using a low energy 1,927 nm non-ablative fractional laser: a retrospective photographic review analysis. Lasers Surg Med. 2020;52:7–12.
14. Saedi N, Petrell K, Arndt K, Dover J. Evaluating facial pores and skin texture after low-energy non-ablative fractional 1440-nm laser treatments. J Am Acad Dermatol. 2013;68:113–8.
15. Brauer JA, Alabdulrazzaq H, Bae YS, Geronemus RG. Evaluation of a low energy, low density, non-ablative fractional 1927 nm wavelength laser for facial skin resurfacing. J Drugs Dermatol. 2015;14:1262–7.
16. Vanaman Wilson MJ, Jones IT, Bolton J, Larsen L, Fabi SG. The safety and efficacy of treatment with a 1,927 nm diode laser with and without topical hydroquinone for facial hyperpigmentation and melasma in darker skin types. Dermatol Surg. 2018;44:1304–10.
17. Kaufmann R, Hartmann A, Hibst R. Cutting and skin-ablative properties of pulsed mid-infrared laser surgery. J Dermatol Surg Oncol. 1994;20:112–8.
18. Pozner JN, Goldberg DJ. Superficial erbium:YAG laser resurfacing of photodamaged skin. Journal of Cosmetic Laser Ther. 2006;8:89–91.
19. Orringer JS, RIttié L, Hamilton T, Karimipour DJ, Voorhees JJ, Fisher GJ. Intraepidermal erbium:YAG laser resurfacing. J Am Acad Dermatol. 2011;64:119–28.
20. Weiss ET, Brauer JA, Anolik R, et al. 1927-nm fractional resurfacing of facial actinic keratoses: a promising new therapeutic option. J Am Acad Dermatol. 2013;68:98–102.
21. Cho S, Lee S, Cho S, Oh S, Chung W, Kang J, et al. Non-ablative 1550-nm erbium-glass and ablative 10600-nm carbon dioxide fractional lasers for acne scars: a randomized split-face study with blinded response evaluation. J Eur Acad Dermatol Venereol. 2010;24:921–5.
22. Sherling M, Friedman PM, Adrian R, Burns JA, Conn H, Fitzpatrick R, et al. Consensus recommendations on the use of an erbium-doped 1550-nm fractionated laser and its applications in dermatologic laser surgery. Dermatol Surg. 2010;36:461–9.
23. Ortiz AE, Goldman MP, Fitzpatrick RE. Ablative CO_2 lasers for skin tightening: traditional versus fractional. Dermatol Surg. 2014;40(Suppl 12):S147–51.
24. Cohen JL, Ross EV. Combined fractional ablative and nonablative laser resurfacing treatment: a split-face comparative study. J Drugs Dermatol. 2013;12:175–8.
25. Regan TD, Uebelhoer NS, Satter E, Ross EV. Depth of tissue ablation and residual thermal damage caused by a pixilated 2,940 nm laser in a swine skin model. Lasers Surg Med. 2010;42:408–11.

How to cite this article: Bernstein EF, Sanzo JF, Wang JY, Cotsarelis SM, DiLeonardo M. Low-fluence treatment with a novel fractionated 2910-nm fiber laser improves photodamage. Lasers Surg Med. 2023;55:35–45. https://doi.org/10.1002/lsm.23624